MOLECULAR IMAGING AND BIOLOGY

Mol Imaging Biol (2019) 21:1107–1116
DOI: 10.1007/s11307-019-01331-8

Published Online: 5 March 2019

WMIS World Molecular Imaging Society

Check for updates

RESEARCH ARTICLE

Non-invasive Use of Positron Emission Tomography to Monitor Diethyl maleate and Radiation-Induced Changes in System x_C^- Activity in Breast Cancer

Milena Čolović,[1,2] Hua Yang,[1] Helen Merkens,[2] Nadine Colpo,[2] François Bénard,[2,3,4] Paul Schaffer[1,4,5]

[1]*Life Sciences Division, TRIUMF, 4004 Wesbrook Mall, Vancouver, BC, V6T 2A3, Canada*
[2]*British Columbia Cancer Research Centre, Vancouver, BC, Canada*
[3]*Molecular Oncology, British Columbia Cancer Research Centre, 675 W 10th Ave, Vancouver, BC, V5Z 1L3, Canada*
[4]*Department of Radiology, Faculty of Medicine, University of British Columbia, Vancouver, Canada*
[5]*Department of Chemistry, Faculty of Science, Simon Fraser University, Vancouver, Canada*

Abstract

Purpose: The system x_C^- transporter is upregulated in cancer cells in response to oxidative stress (OS). 5-[^{18}F]fluoroaminosuberic acid ([^{18}F]FASu) has been reported as a novel positron emission tomography (PET) imaging agent, targeting system x_C^-. The goal of this study was to evaluate the utility of [^{18}F]FASu in monitoring cellular response to diethyl maleate (DEM) and radiation-induced OS fluctuations.

Procedures: [^{18}F]FASu uptake by breast cancer cells was studied in correlation to OS biomarkers: glutathione (GSH) and reactive oxygen species (ROS), as well as transcriptional and translational levels of xCT (the functional subunit of x_C^-). System x_C^- inhibitor, sulfasalazine (SSZ), and small interfering RNA (siRNA) knockdown were used as negative controls. Radiotracer uptake was evaluated in three breast cancer models: MDA-MB-231, MCF-7, and ZR-75-1, at two-time points (1 h and 16 h) following OS induction. *In vivo* [^{18}F]FASu imaging and biodistribution were performed using MDA-MB-231 xenograft-bearing mice at 16 and 24 h post-radiation treatment.

Results: [^{18}F]FASu uptake was positively correlated to intracellular GSH and *SLC7A11* expression levels, and radiotracer uptake was induced both by radiation treatment and by DEM at time points longer than 3 h. In an *in vivo* setting, there was no statistically significant uptake difference between irradiated and control tumors.

Conclusion: [^{18}F]FASu is a specific system x_C^- PET radiotracer and as such it can be used to monitor system x_C^- activity due to OS. As such, [^{18}F]FASu has the potential to be used in therapy response monitoring by PET. Further optimization is required for *in vivo* application.

Electronic supplementary material The online version of this article (https://doi.org/10.1007/s11307-019-01331-8) contains supplementary material, which is available to authorized users.

Correspondence to: François Bénard; *e-mail:* fbenard@bccrc.ca, Paul Schaffer; *e-mail:* pschaffer@triumf.ca

Key words: Oxidative stress, FASu, Positron emission tomography, Breast cancer, Cystine transporter, Glutathione, Radiation therapy

Introduction

Reactive oxygen species (ROS) modulation plays a crucial role in maintaining cellular redox homeostasis [1]. Cancer cells have a high ROS burden due to metabolic and signaling aberrations compared with normal cells [2]. This heavy ROS burden promotes tumor growth and proliferation by increasing genomic instability and activating pro-oncogenic signaling pathways [1, 3]. In order to cope with the ROS burden, cancer cells elevate antioxidant defense mechanisms [4].

Many studies show a correlation between increased OS and overexpression of system x_C^-, the cystine/glutamate antiporter [5–8]. This amino acid transporter is expressed at low levels in most tissues and becomes upregulated under OS [6]. It consists of two components: a heavy chain subunit, 4F2hc (*SCL2A3*), and a small chain subunit, xCT (*SLC7A11*), the latter of which is unique to system x_C^- and confers substrate specificity [9]. System x_C^- plays an important role in OS modulation as it is the primary cellular source of cystine [10], which upon import into the cell is reduced to cysteine, the rate-liming precursor for glutathione (GSH) synthesis [9]. GSH, as the major cellular antioxidant, neutralizes free radicals as well as reactive oxygen and nitrogen species [5, 8, 9]. By upregulating system x_C^-, cancer cells enhance cystine uptake in order to maintain appropriate antioxidant levels within the cell. The strategy of increasing antioxidant production and lowering ROS levels has proven to be beneficial for cancer stem cells (CSCs) in the context of radiotherapy resistance [4].

The vital role system x_C^- plays in ROS modulation makes it an appealing target for cancer therapy and positron emission tomography (PET) tracer development. The activity of system x_C^- exclusively depends on its light chain subunit, xCT [9], which was explored by other groups as a potential target for PET imaging [11, 12]. Gout- et al. have demonstrated that pharmacological inhibition of xCT-arrested tumor growth in rats [13]. Furthermore, it has been shown that tumors with increased xCT activity are associated with resistance to chemotherapy and that inhibition of xCT sensitizes cancer cells to chemotherapeutic agents such as etoposide [4, 14], doxorubicin [15, 16], celastrol, and gemcitabine [17].

In the absence of druggable molecular targets, there is a lack of targeted therapies for triple-negative breast cancer (TNBC). Chemo- and radiation-therapy remain as the only treatment options; however, they have had limited success when compared with non-TNBC subtypes [18]. xCT is overexpressed in one-third of all TNBCs *in vivo* [19] and therefore may pose a useful diagnostic target for cancer imaging [5, 20]. With this in mind, we have previously reported the synthesis of a PET radiotracer 5-[^{18}F]fluoroaminosuberic acid ([^{18}F]FASu) [5, 20], which is specific to system x_C^- and demonstrated to have higher uptake in TNBC xenografts when compared with non-TNBC subtypes [5]. The goal of this study was to evaluate whether [^{18}F]FASu is an indicator of xCT expression in response to oxidative stress *in vitro* and *in vivo*.

Materials and Methods

General

All chemicals obtained commercially were used without further modifications unless otherwise indicated. [^{18}F]FASu was prepared as previously reported [6, 19]. Quality control of the radiosynthesis was performed by HPLC (Agilent 1200 equipped with a diode array and Raytest GABI Star scintillation detector). Cell irradiation was performed using an XRAD 320 X-ray machine (Precision X-ray Inc.). Small animal imaging experiments were performed using an Inveon Multi-Modality μPET/X-ray computed tomography (CT) system (Siemens Healthineers, USA). Localized tumor radiation treatment was performed on a Small Animal Radiation Research Platform (SARRP, Xstrahl Limited). Radioactivity of samples was measured by a calibrated Perkin Elmer Wizard 2480 gamma counter.

In vitro uptake experiments, siRNA knockdown, Western blotting, glutathione, and ROS level measurements were performed according to previously established or commercially available protocols. Detailed *in vitro* and animal experimentation protocols, along with statistical analysis methods of the data, are outlined in the electronic supplementary material (ESM). All animal studies were conducted in accordance with the guidelines established by the Canadian Council on Animal Care and approved by the Animal Ethics Committee of the University of British Columbia. All data are expressed as mean ± SD with data considered statistically significant when p value was less than 0.05.

Results

[^{18}F]FASu Uptake, SLC7A11, and xCT Expression Vary in Response to Prolonged DEM Treatment

To confirm, [^{18}F]FASu uptake is related to system x_C^- activity, and to investigate response to OS, we used siRNA to knockdown xCT mRNA (*SLC7A11*) expression and

examined both *SLC7A11* and xCT expression levels and [^{18}F]FASu uptake in MDA-MB-231, a triple-negative breast cancer (TNBC) cell line, in the presence and absence of the OS-inducer diethyl maleate (DEM). Figure 1a shows that siRNA knockdown induced an 8.7-fold decrease in the expression of *SLC7A11* gene. Twenty-four-hour treatment with DEM resulted in increases in intracellular levels of *SLC7A11* in untreated (no siRNA), control ("scramble" siRNA)- and xCT siRNA-treated samples compared with non-DEM-treated samples, indicating the positive correlation between OS and *SLC7A11* expression (Fig. 1a).

Cellular uptake of [^{18}F]FASu was reduced by 50 % in cultures treated with xCT siRNA when compared with controls (Fig. 1b). In the presence of DEM, [^{18}F]FASu uptake increased significantly as compared with the untreated sample, with the effect being the greatest in the case when no siRNA was added ($p < 0.0001$ for no siRNA and control siRNA samples, and $p = 0.0013$ for xCT siRNA-treated sample). The system x_C^- inhibitor, sulfasalazine (SSZ), completely blocked [^{18}F]FASu uptake by MDA-MB-231 cells (Fig. 1b). These results indicate that [^{18}F]FASu uptake is increased by DEM induction of system x_C^-.

Western blot analysis on these MDA-MB-231 cell lysates confirmed that translational xCT expression directly reflects changes in the transcriptional expression of *SLC7A11* (Fig. 1c), while actin expression did not fluctuate. Furthermore, DEM-induced xCT expression across board, in accordance with the qPCR results, showing that mRNA and protein expression both increase as a consequence of OS induction.

System x_C^- Activity Changes with DEM Incubation in a Time-Dependent Manner

Building on our previous results [5], we performed a time-dependent study by inducing OS with 0.1 mM DEM. No significant change in [^{18}F]FASu uptake was observed in MDA-MB-231 cells within the first 1.5 h of treatment (Fig. 2a; $p = 0.89$ for 1.5 h time point and $p = 0.97$ for 45 min time point). However, after 3 h, tracer uptake increased by 39.9 ± 14.2 % as compared with the untreated control ($p < 0.0001$) and continued to increase over time. At 15 h, [^{18}F]FASu uptake was 137.9 ± 26.4 % higher than that of the untreated sample ($p < 0.0001$). [^{18}F]FASu uptake remained unchanged in the presence of system x_C^- inhibitor SSZ irrespective of the duration of DEM treatment. The results suggest that system x_C^- activity continuously increases in the presence of DEM.

System x_C^- Response to Short (1 h) versus Long (Overnight) DEM Treatment in MDA-MB-231 Cells

After 1 h treatment with DEM, *SLC7A11* expression, [^{18}F]FASu uptake and intracellular glutathione (GSH) content (Fig. 2b, c, and d, respectively) did not vary significantly from the untreated controls. However, the mean fluorescence intensity increased significantly when using CM-H_2DCFDA dye as an indicator, suggesting an increased ROS burden in treated MDA-MB-231 cells (Fig. 2e). Conversely, prolonged treatment with DEM resulted in transcriptional upregulation of *SLC7A11* ($p < 0.0001$) increased [^{18}F]FASu uptake by 56.3 ± 26.1 % ($p < 0.001$) and GSH content by 40.5 ± 25.8 % ($p < 0.05$, Fig. 2b-d); while ROS levels were noted to return to baseline (Fig. 2e). Evidently, shorter exposure to the stressor DEM was not sufficient to result in changes in *SLC7A11* mRNA expression, system x_C^- activity, or GSH production. On the other hand, prolonged exposure to DEM caused the cells under study to respond by increasing their GSH production and upregulating *SLC7A11* expression.

Determination of xCT Expression, GSH and ROS Content, and [^{18}F]FASu Uptake in Additional, ER+/PR+, Breast Cancer Cell Lines after 1 h and Overnight Treatment with DEM

With preliminary mRNA expression, [^{18}F]FASu uptake, GSH and ROS response data in hand, we then expanded our

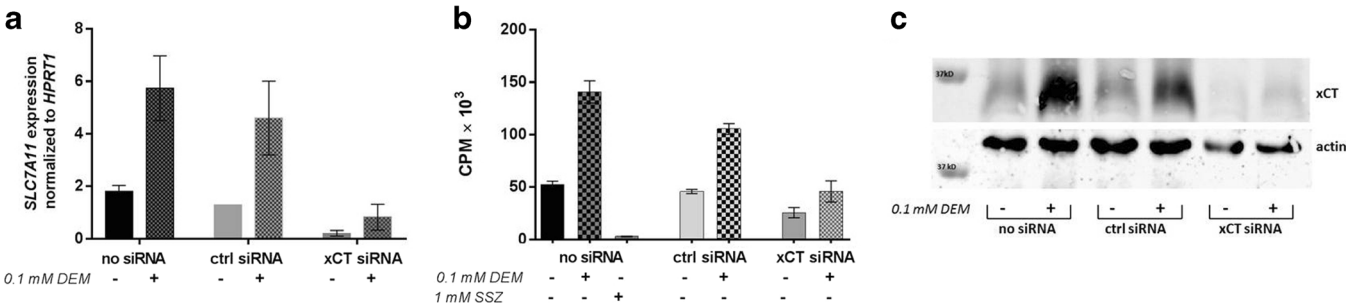

Fig.1 **a** Absolute qPCR quantitation of *SLC7A11* expression after 48 h siRNA knockdown compared with no siRNA or control siRNA in MDA-MB-231 cells. Twenty-four-hour treatment with diethyl maleate (DEM, 0.1 mM) caused upregulation of *SLC7A11* expression. **b***In vitro* 1 h uptake of [^{18}F]FASu in MDA-MB-231 cells increased after 24 h exposure to DEM and xCT siRNA knockdown. **c** Western blot analysis of siRNA-treated MDA-MB-231 cell lysates showed knockdown of xCT expression in xCT siRNA-treated sample and overexpression of xCT in DEM-treated samples. The actin blot was used as loading control. Uncropped blots are shown in Suppl. Fig. S2.

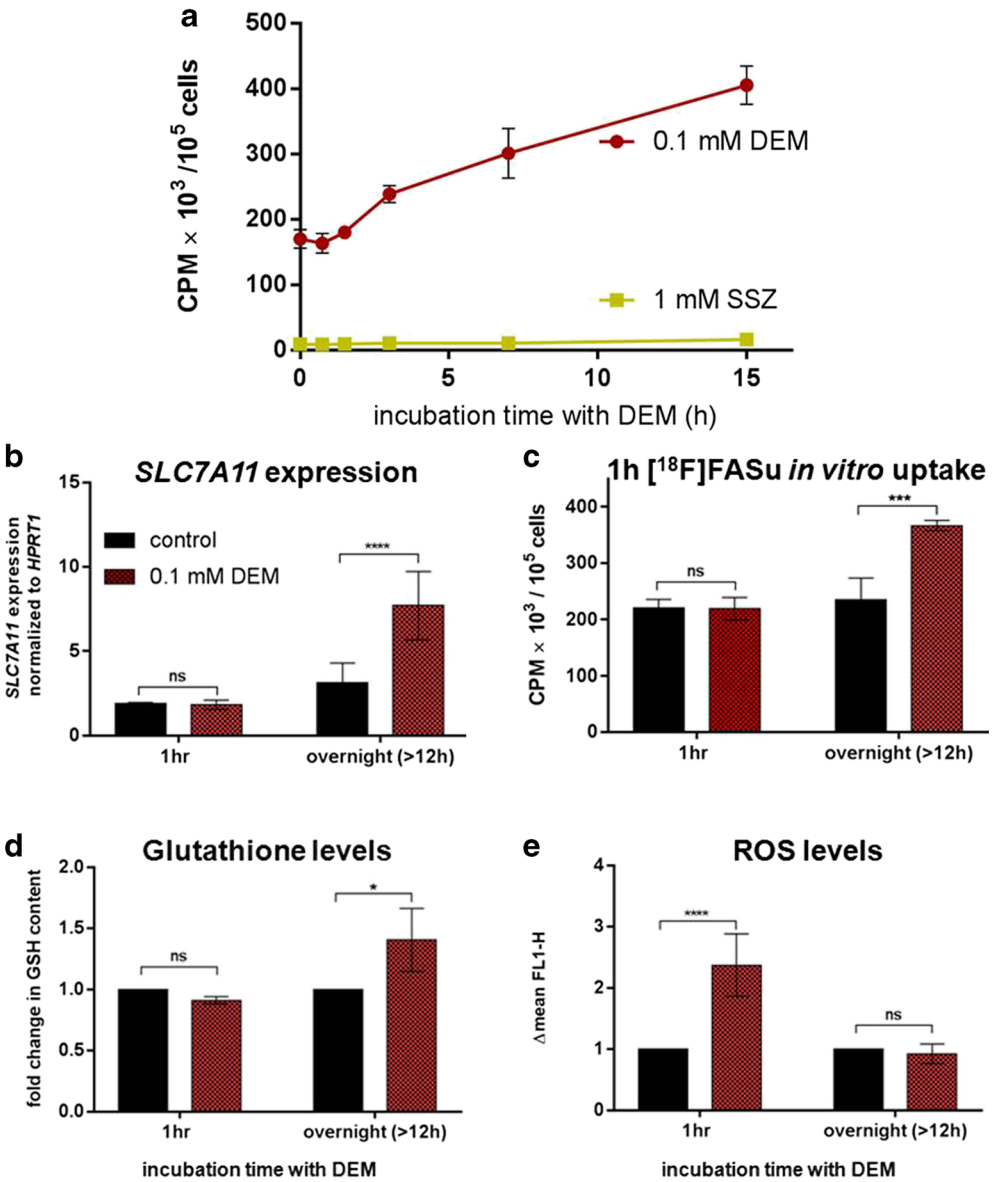

Fig. 2 **a** One hour *in vitro* [^{18}F]FASu uptake by MDA-MB-231 cells (—●—) after varying duration of treatment with DEM (0.1 mM). The uptake was blocked by SSZ (1 mM) (—■—). **b***HPRT1*-normalized *SLC7A11* expression in MDA-MB-231 cells with and without 1 h or overnight incubation with DEM. **c** One hour *in vitro* uptake of [^{18}F]FASu in MDA-MB-231 cells with and without 1 h or overnight incubation with DEM. **d** Intracellular GSH levels increased after overnight treatment with DEM (*$p < 0.05$), but 1 h DEM incubation did not cause the difference compared with the control sample. **e** ROS levels measured as mean CM-H_2DCFDA fluorescence increased significantly (****$p < 0.0001$) after 1 h co-incubation with DEM but returned to the same level as the untreated control sample in the case of overnight incubation.

cohort of cell lines to examine [^{18}F]FASu uptake in two different ER+/PR+ cell lines, MCF-7, and ZR-75-1.

As shown in Fig. 3a, overnight treatment with DEM resulted in overexpression of xCT in all three breast cancer cell lines. Moreover, our results indicate that 1 h incubation with DEM, SSZ, or the two in combination caused no significant differences in GSH content (Fig. 3c). Similarly, [^{18}F]FASu uptake did not change significantly when compared with untreated controls (Fig. 3b). When cells were treated with DEM overnight, GSH levels increased in all three cell lines (Fig. 3c, $p < 0.0001$), as did [^{18}F]FASu uptake (Fig. 3b, $p < 0.05$ in the case of MDA-MB-231, $p < 0.01$ for the hormone receptor-positive cells). SSZ was shown to block [^{18}F]FASu uptake in all cases indicating specific uptake *via* system x_C^-. GSH levels decreased when xCT was blocked by SSZ incubation overnight, and they decreased even further when both OS-inducer DEM and xCT-inhibitor SSZ were present together in the media overnight (Fig. 3c).

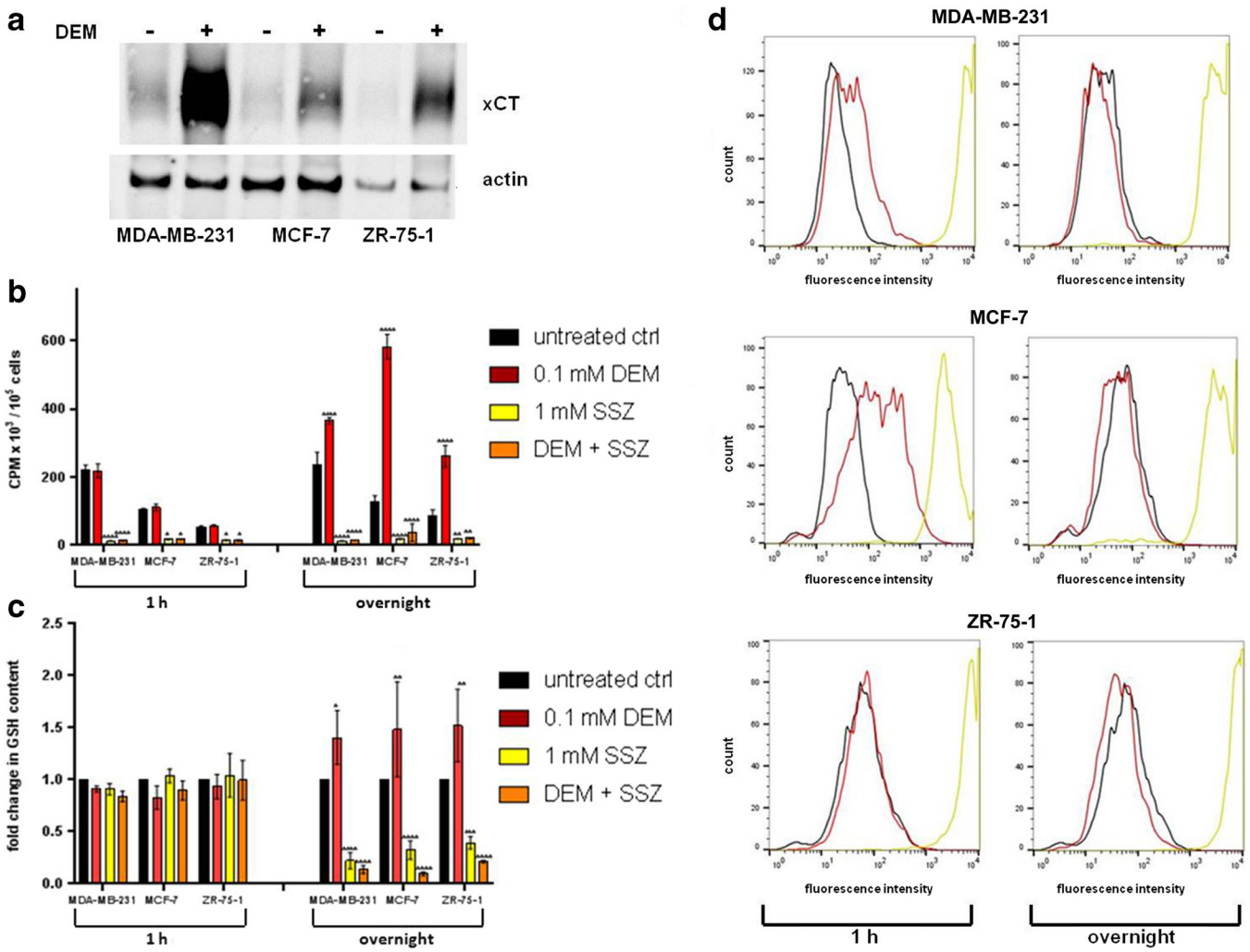

Fig. 3 **a** Western blot showing xCT and actin expression levels in all three cell lines after overnight incubation with 0.1 mM DEM. Uncropped blots are shown in the ESM, Suppl. Fig. S3. **b***In vitro* [^{18}F]FASu uptake did not change after 1 h incubation with DEM, while it was blocked by SSZ regardless of whether DEM is present (****$p < 0.0001$, *$p < 0.05$). Overnight treatment with DEM resulted in increased [^{18}F]FASu uptake (****$p < 0.0001$). The tracer uptake was blocked in the presence of SSZ (****$p < 0.0001$, **$p < 0.01$). **c** GSH levels remained constant in all three breast cancer cell lines after 1 h treatment with OS-inducer DEM, in the presence and absence of SSZ. One hour treatment with SSZ did not change intracellular GSH levels as compared with untreated control samples ($p > 0.05$). Overnight treatment with DEM, SSZ, or DEM and SSZ influenced GSH levels significantly in all three breast cancer cell lines. DEM promotes GSH synthesis, while the presence of SSZ in the samples caused GSH depletion in all cells. **d** Flow cytometry CM-H_2DCFDA staining showed a partial shift in fluorescence peak after 1 h treatment with DEM (red) in MDA-MB-231 and MCF-7, but not in ZR-75-1 cells. Blocking system x_C^- with SSZ resulted in a twofold peak shift in all cell lines (yellow), regardless of the incubation duration. Control cells are presented as black lines.

Using flow cytometry, both MCF-7 and MDA-MB-231 cells demonstrated increased ROS burden after 1 h incubation with DEM, whereas ZR-75-1 cells showed no corresponding fluorescent peak shift (Fig. 3d). In the presence of SSZ, significantly higher fluorescence intensity was observed in all three cell lines regardless of treatment duration (1 h and overnight), meaning that the treated cells experienced higher ROS levels. After prolonged DEM incubation, none of three cell lines demonstrated fluorescent peak shift, which could be explained by increased GSH production (Fig. 3c).

Ex vivo qPCR and Western Blot Experiments

qPCR studies on breast cancer xenografts show the same pattern of *SLC7A11* expression, with MDA-MB-231 having the highest xCT mRNA expression as compared with MCF-7 and ZR-75-1 (Fig. 4a–b) tumors. In order to investigate whether the transcriptional expression levels are correlated with protein expression levels, we performed Western blots on cell lines and tumor lysates. Notably, when comparing two commercially available anti-xCT antibodies (Abcam and Cell Signaling Technologies (CST)), we found that the most

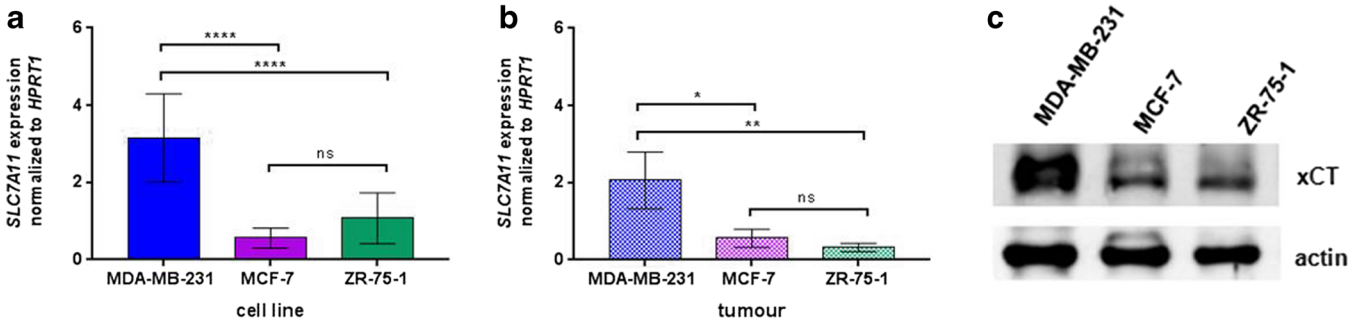

Fig. 4 **a** MDA-MB-231 cells (blue bar) expressed *SLC7A11* mRNA at significantly higher levels *in vitro* than MCF-7 and ZR-75-1 cell lines (purple and green bars, respectively, $^{****}p < 0.0001$). **b***SLC7A11* expression in harvested MDA-MB-231 tumors (blue bar) was higher than in the other two tumors (MCF-7 in purple and ZR-75-1 in green, $^{*}p < 0.05$, $^{**}p < 0.01$). There was no statistically significant difference between *SLC7A11* mRNA levels between MCF-7 and ZR-75-1 ($p > 0.05$). **c** Western blot of MDA-MB-231, MCF-7 and ZR-75-1 tumor lysates indicated that MDA-MB-231 tumors had higher xCT expression than the two hormone receptor-positive tumors. Uncropped blots are shown in the ESM, Suppl. Fig. S5.

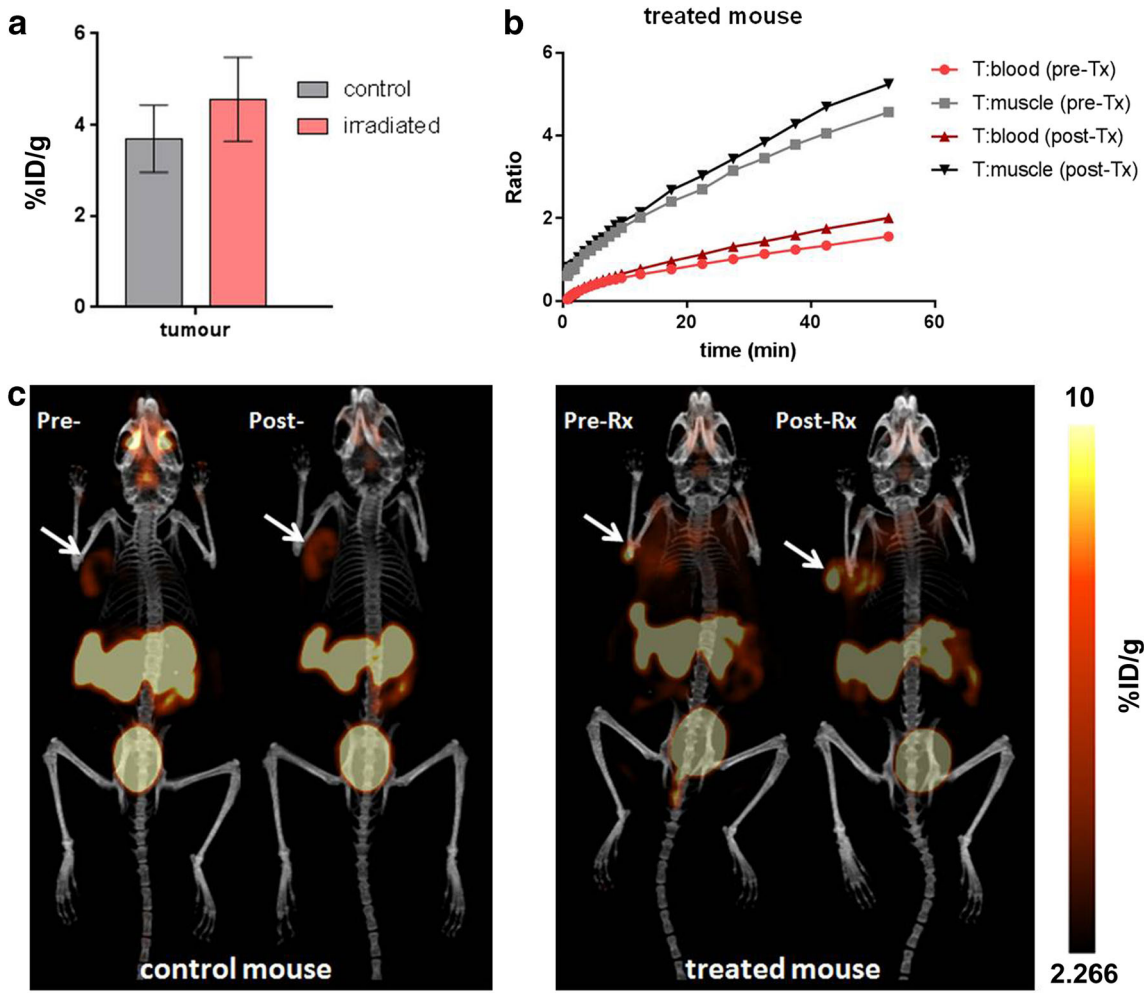

Fig. 5 **a** Biodistribution data indicate no statistically significant differences between control ($n = 6$) and treated ($n = 9$) groups. **b** Time-activity curve (TAC) of tumor-to-nontarget ratios in a mouse that underwent localized radiation treatment. **c** MDA-MB-231 tumors (white arrows) are visualized with [^{18}F]FASu-PET 55 min post-injection. Acquisition time was 10 min. The same animal is depicted twice, for both the control and the treated mouse, with the images being the pre- and post-therapy.

Table 1. Biodistribution data of [^{18}F]FASu at 1 h post-injection collected at 24 h post-radiation therapy of MDA-MB-231 xenografts in NRG mice

	Control, $n = 6$		Irradiated, $n = 9$	
Organs (tissues)	% ID/g	± SD	% ID/g	± SD
Blood	0.63	0.11	0.65	0.20
Fat	0.04	0.02	0.05	0.01
Ovaries	2.97	0.75	3.32	1.41
Uterus	4.36	1.87	4.20	1.80
Small intestine	1.47	0.46	1.50	0.42
Stomach	1.92	0.51	2.02	0.91
Pancreas	26.03	1.28	27.42	3.52
Spleen	1.92	0.65	2.27	1.28
Liver	0.97	0.21	0.78	0.23
Adrenal glands	0.71	0.23	0.74	0.25
Kidneys	20.51	3.61	23.21	9.99
Heart	0.26	0.05	0.27	0.08
Lungs	1.84	0.23	2.17	0.39
MDA-MB-231 tumor	3.70	0.74	4.56	0.92
Muscle	0.22	0.06	0.21	0.06
bone	1.03	0.17	0.88	0.24
brain	0.08	0.01	0.10	0.01
	Ratio	± SD	Ratio	± SD
Tumor/blood	5.92	0.82	7.33	1.42
Tumor/fat	93.16	26.39	102.05	23.87
Tumor/muscle	17.15	3.77	22.82	4.46
Tumor/brain	44.49	8.66	47.53	5.22

consistent results were obtained then using the antibody sourced from CST. While both Abcam and CST anti-xCT antibodies recognize the recombinant human xCT protein (Suppl. Fig. S4, see ESM), the Abcam antibody revealed a 55 kDa band that did not change in response to any treatment, while the CST antibody recognized a 35 kDa band that changed in a manner consistent with treatment (±DEM or xCT siRNA). Western blot indicated the highest xCT expression in MDA-MB-231 (Fig. 3a and 4c), which was consistent with transcriptional *SLC7A11* levels determined by our qPCR experiments (Fig. 4a-b). Overnight treatment with DEM increased expression of xCT in all three cell lines (Fig. 3a).

In vivo Radiotherapy and [^{18}F]FASu-PET/CT Imaging

In vivo uptake of [^{18}F]FASu uptake in MDA-MB-231 tumors was examined before and after localized radiation therapy in NRG mice at 1 h post-injection and 24 h post-treatment (Fig. 5). While the overall tracer biodistribution

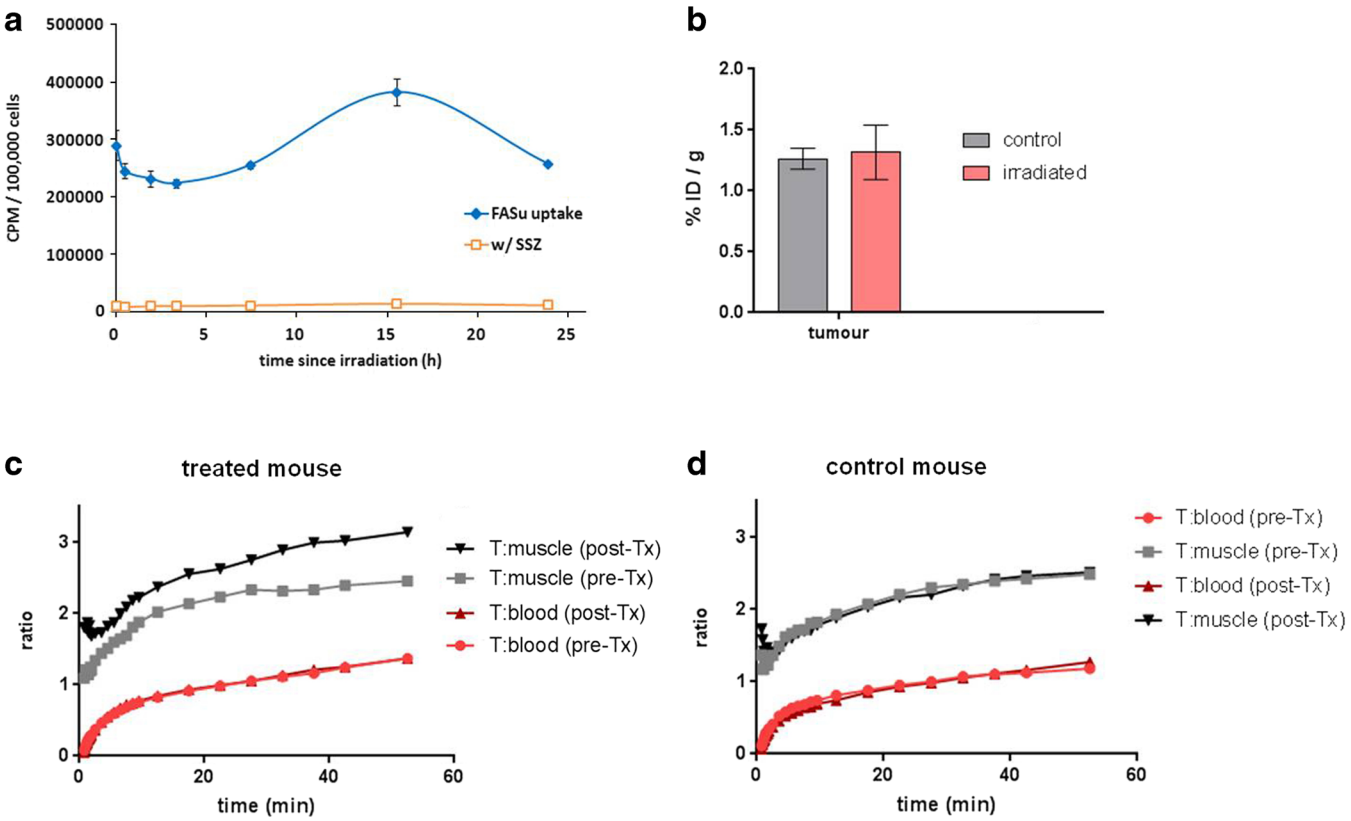

Fig. 6 **a** *In vitro* [^{18}F]FASu uptake (◊) peaked at 16 h time point following 2 Gy irradiation of MDA-MB-231 cells. Sulfasalazine (SSZ, 1 mM) treatment was used as a negative control for each time point (□). **b** Biodistribution data indicated no statistically significant differences between MDA-MB-231 tumor uptake in control ($n = 6$) and treated ($n = 10$) groups. **c** TAC of tumor-to-nontarget ratios in a mouse that underwent localized radiation treatment. **d** TAC of tumor-to-nontarget ratios in the mouse that underwent mock treatment.

Table 2. Biodistribution data of [^{18}F]FASu at 1 h post-injection collected at 16 h post-radiation therapy of MDA-MB-231 xenografts in NRG mice

	Control, $n = 6$		Irradiated, $n = 10$	
Organs (tissues)	% ID/g	± SD	% ID/g	± SD
Blood	0.45	0.09	0.54	0.12
Fat	0.06	0.02	0.05	0.02
Ovaries	2.32	1.91	2.01	1.07
Uterus	3.05	1.16	2.84	0.97
Small intestine	1.35	0.26	1.19	0.31
Stomach	1.40	0.49	1.57	0.73
Pancreas	23.53	2.76	28.77	8.25
Spleen	1.78	0.48	1.32	0.41
Liver	0.73	0.19	0.69	0.17
Adrenal glands	0.35	0.14	0.97	1.06
Kidneys	16.42	4.89	20.52	6.46
Heart	0.19	0.04	0.29	0.11
Lungs	1.74	0.22	2.21	0.77
MDA-MB-231 tumor	1.27	0.09	1.32	0.22
Muscle	0.20	0.04	0.24	0.12
Bone	0.79	0.30	0.56	0.21
Brain	0.09	0.02	0.11	0.04
	Ratio	± SD	Ratio	± SD
Tumor/blood	2.88	0.42	2.48	0.44
Tumor/fat	23.39	7.20	26.97	7.06
Tumor/muscle	6.43	0.95	6.44	2.50
Tumor/brain	15.16	2.05	12.40	3.46

did not change significantly as a consequence of localized radiotherapy (Fig. 5a, Table 1), tumor uptake did increase from 3.70 ± 0.74 to 4.56 ± 0.92 %ID/g, in non-treated *versus* treated group, respectively. This difference is not statistically significant ($p = 0.078$); however, tumor-to-background tissue ratios did increase sufficiently and improved image contrast (Fig. 5b-c, Table 1). Tumor-to-blood and tumor-to-muscle ratios continued increasing throughout the duration of the dynamic scan.

[^{18}F]FASu as a Gauge for Oxidative Stress Level Monitoring in TNBC

To understand how [^{18}F]FASu uptake changed over time after radiation exposure, we irradiated cells with a sublethal dose of X-ray radiation ($LD_{50} = 2$ Gy, previously established in our lab) and measured tracer uptake at different time points. We found that [^{18}F]FASu uptake gradually increased 5 h after irradiation, peaking at 16 h where it was 32.0 ± 14.4 % higher than that of the control cells ($p < 0.0001$) (Fig. 6a). At the final time point of 24 h post-irradiation, tracer uptake returned to the level of the control (non-irradiated) cells.

In vivo Radiotherapy and [^{18}F]FASu-PET/CT Imaging—Part 2

We examined *in vivo* [^{18}F]FASu uptake 16 h after localized irradiation of MDA-MB-231 tumors but did not observe significant tracer uptake differences between treated and control groups (Fig. 6b, Table 2). Tumor-to-nontarget ratios were higher following radiation treatment as compared with the baseline levels (Fig. 6c). Moreover, the increase in tumor-to-muscle ratios over time was not observed in the mouse that received mock treatment (Fig. 6d).

Table 3. Tumor weight and [^{18}F]FASu uptake data at 1 h post-injection from the two biodistribution studies collected at 24 h (study #1) and 16 h (study #2) post-radiation (post-Rx) therapy of MDA-MB-231 xenografts in NRG mice. The control tumors were harvested from the animals that received mock treatment

	Study #1		Study #2	
	24 h post-Rx		16 h post-Rx	
	All tumors, $n = 15$		All tumors, $n = 16$	
	Mean	± SD	Mean	± SD
Tumor weight (g)	0.5620	0.1996	0.2345	0.0892
****p value < 0.0001				
	Control tumors, $n = 6$		Control tumors, $n = 6$	
	Mean	± SD	Mean	± SD
Tumor weight (g)	0.4362	0.0764	0.2032	0.0566
*p value = 0.0215				
Tumor uptake (%ID/g)	3.70	0.74	1.27	0.09
****p value < 0.0001				

Discussion

We hypothesize that system x_C^-, a cystine/glutamate anti-porter, with a very narrow natural substrate binding profile yet sufficient upregulation in disease could be a useful target for PET imaging [5, 20]. System x_C^- has been shown to be upregulated under OS, which plays an important role in cancer differentiation and proliferation [1, 4, 6]. A specific radiotracer driven by OS may have value in detection, staging, and therapy response monitoring. It has been reported previously that TNBC has higher xCT expression and cystine consumption, which supports the potential utility of [^{18}F]FASu-PET in clinical breast cancer management [5, 19].

In an attempt to address the question of [^{18}F]FASu uptake specificity, we have previously reported higher [^{18}F]FASu uptake both *in vitro* and *in vivo* in HEK293T::xCT cells and tumors as compared with the wild-type HEK293 [5]. However, we were unable to prove the direct correlation to xCT protein expression levels at that time due to the lack of a reliable and specific anti-xCT antibody [21]. With the Western blot, siRNA knockdown and qPCR studies presented herein, we are convinced that the 35 kDa band recognized by the antibody from CST represents the true functional human xCT protein. This finding contradicts a previously drawn conclusion that the 50–55 kDa band is the functional xCT [22], but is in concordance with more recently published findings with in-house made antibodies by multiple groups [21, 23–26]. Our specificity study in Fig. 1 showed direct correlation of tracer uptake and *SLC7A11* and xCT levels in MDA-MB-231 cells. With this study, we have thus established a link between transcriptional and translational levels of xCT and the transport activity of system x_C^-, which is reflected in [^{18}F]FASu uptake.

It was previously demonstrated that [^{18}F]FASu uptake and GSH levels increase with DEM treatment [5], presumably due to increased ROS which resulted in system x_C^- upregulation. To understand the changes reflected upon these biomarkers when OS is artificially induced by DEM, and also to understand the time frame for those changes to occur, we investigated GSH, ROS, *SLC7A11*, and [^{18}F]FASu uptake at various time points after DEM treatment. First, we performed an uptake study in which the incubation time with 0.1 mM DEM was varied. Figure. 2a shows that system x_C^- activity continuously increased in the presence of DEM, as reflected by increase in cellular uptake of [^{18}F]FASu. There was upregulation in system x_C^- expression or activity in cells for incubation duration superior to 3 h.

Utilizing the TNBC cell line, MDA-MB-231, we wanted to compare cellular markers of OS, GSH, and ROS levels, in relation to xCT mRNA expression and [^{18}F]FASu uptake at 1 and 16 h. Not surprisingly, a 1 h treatment with DEM did not result in increased tracer uptake or *SLC7A11* expression in MDA-MB-231 cells. In fact, a rapid increase in crude ROS levels was observed *via* fluorescence assay with little to no effect on GSH levels. On the contrary, at the longer time point, *SLC7A11* expression, [^{18}F]FASu uptake, and GSH all increased substantially, whereas ROS levels were not observed to be different from untreated controls. We suspect ROS returned to basal levels due to an increase in antioxidant (glutathione) production following xCT gene (*SLC7A11*) and x_C^- protein upregulation.

When we expanded the cohort to compare three breast cancer cell lines and assessed antioxidant load and [^{18}F]FASu uptake, we found that similarly to MDA-MB-231, ER+/PR+ cell lines showed the same positive correlation between system x_C^- activity and GSH levels. Regardless of the molecular signature of the breast cancer cells, it seems that increase in GSH production is enabled due to system x_C^- upregulation (Fig. 3a-c). Correspondingly, no fluorescent peak shift was observed after prolonged incubation of the cells with DEM (Fig. 3d). We hypothesize that cells adjust to the presence of the OS inducer in their media, and maintain increased antioxidant capacity in order to balance the ROS increase. Blocking system x_C^- with xCT inhibitor SSZ had the smallest impact on ZR-75-1 cells (Fig. 3b-c), as reflected in lower percentage of [^{18}F]FASu uptake blocking (78 % uptake inhibition compared with 86 % and 94 % in MCF-7 and MDA-MB-231 cells, respectively) and lesser decrease in amount of GSH (60 % compared with 68 % and 78 % in MCF-7 and MDA-MB-231 cells, respectively), suggesting some alternative, unknown mode of cystine uptake with ZR-75-1. Similarly, flow cytometry results with ZR-75-1 differed from those with MCF-7 and MDA-MB-231 cells (Fig. 3d). No fluorescent peak shift was observed after 1 h treatment with DEM, indicating no detectable increase in ROS burden in ZR-75-1 cells. Evidently, OS compensation is taking place at a different rate in this cell line, but under a mechanism that remains unclear.

When we compared *in vitro SLC7A11* mRNA abundance to the one extracted from harvested tumors, we found that the TNBC has the highest *SLC7A11* expression both *in vitro* and *ex vivo* (Fig. 4a-b), consistent with MDA-MB-231 cells having higher [^{18}F]FASu uptake than MCF-7 and ZR-75-1 (Fig. 3b). Additionally, we have also previously demonstrated that MDA-MB-231 tumors have the highest [^{18}F]FASu uptake *in vivo* as compared with MCF-7 and ZR-75-1 [5]. Western blot analysis demonstrated that xCT protein expression levels were the greatest in the triple-negative cells and tumors, MDA-MB-231 (Fig. 3a and 4c, respectively).

Having established a correlation between [^{18}F]FASu and biomarkers associated with OS, we wanted to determine the potential for [^{18}F]FASu to serve as a non-invasive gauge of OS *via* PET. In order to test this hypothesis, *in vitro* experiments were performed in which tracer uptake was determined in irradiated MDA-MB-231 cells at multiple time points. These studies (Fig. 6a) indicated that [^{18}F]FASu uptake achieved maximal uptake at 16 h post-irradiation, and decreased back to base levels by the 24 h time point. With cell data in support of our hypothesis, we then measured [^{18}F]FASu uptake in MDA-MB-231 tumor-bearing NRG mice before and after localized radiation therapy. Images at 16 h post-radiotherapy showed no significant differences between [^{18}F]FASu uptake of treated *versus* control mice (Fig. 6b, 1.32 ± 0.22 and 1.27 ± 0.09 %ID/g, $p = 0.590$). An analysis of tumor uptake at 24 h post-irradiation also did not demonstrate statistically significant difference in tracer uptake between treated and untreated animals (4.56 ± 0.92 and 3.70 ± 0.74 %ID/g, $p = 0.078$). Despite this, time-activity curves from the dynamic scans revealed an increase in tumor-to-muscle ratios after radiation therapy, while this phenomenon was not observed in the control tumor (Fig. 6c, d). Tumor-to-blood ratios remained unchanged on baseline and follow-up scans for both treated and control tumors. It should be noted that there were significant differences in baseline [^{18}F]FASu uptake in the MDA-MB-231 tumor between the two imaging studies, and we are examining extenuating factors that may contribute to these differences, including but not limited to differences in tumor mass between subjects (Table 3, $p < 0.0001$), and cell treatment methods, particularly in the case of such an aggressive cell line as MDA-MB-231.

Studies are underway to eliminate potential sources of variability in an effort to establish whether radiation-based treatment may be correlated between *in vitro* and *in vivo* settings. Specifically, additional studies will seek to evaluate *in vivo* [^{18}F]FASu tumor uptake at varying time points after localized radiation therapy, along with altering radiation doses, with the goal to evaluate the potential to use [^{18}F]FASu-PET to monitor tumor response to radiation therapy. These results will be reported under separate cover.

Conclusions

In summary, we found that intracellular GSH levels directly reflect changes in the system x_C^- activity and support our hypothesis that [^{18}F]FASu could be used as a tool to monitor the cystine transporter activity which is a reflection of intracellular OS burden. Work is currently under way to better understand the interplay of these factors *in vivo*. Preliminary animal PET/CT studies with [^{18}F]FASu demonstrated a notable increase in tumor-to-muscle ratios on dynamic time-activity curves, but did not result in significant differences in average whole-tumor uptake post-radiotherapy. Additional studies are under way in order to determine the ideal post-irradiation follow-up time point for imaging in an effort to determine how changes in x_C- in response to OS could enable the use of PET to better understand the role of this transporter in cancer and other OS-related diseases.

Acknowledgments. We thank The British Columbia Cancer Research Centre Bénard laboratory staff, Iulia Dude, Dr. Jutta Zeisler, and Dr. Carlos Uribe, and Sorenson laboratory post-doctoral fellow Dr. Bo Rafn, for their technical help. We also thank Drs. Donald Yapp, Krista Chung, Nelson Wong, and Youssef Ben Bouchta for their assistance during tumor radiation therapy experiment on the SARRP machine.

Funding Information. This work was supported by funds from CIHR (201403COP, 329895) and NSERC CREATE IsoSiM Stipend, grant no. 448110, competition year 2014. TRIUMF receives federal funding *via* a contribution agreement with the National Research Council of Canada.

Compliance with Ethical Standards

Conflict of Interest

The authors declare that they have no conflict of interest.

References

1. Gorrini C, Harris IS, Mak TW (2013) Modulation of oxidative stress as an anticancer strategy. Nat Rev Drug Discov 12:931–947
2. Cairns RA, Harris IS, Mak TW (2011) Regulation of cancer cell metabolism. Cancer 11:85–95
3. Hanahan D, Weinberg RA (2011) Hallmarks of cancer: the next generation. Cell 144:646–674
4. Diehn M, Cho RW, Lobo NA, Kalisky T, Dorie MJ, Kulp AN, Qian D, Lam JS, Ailles LE, Wong M, Joshua B, Kaplan MJ, Wapnir I, Dirbas FM, Somlo G, Garberoglio C, Paz B, Shen J, Lau SK, Quake SR, Brown JM, Weissman IL, Clarke MF (2009) Association of reactive oxygen species levels and radioresistance in cancer stem cells. Nature 458:780–783
5. Yang H, Jenni S, Čolović M et al (2017) ^{18}F-5-fluoroaminosuberic acid as a potential tracer to gauge oxidative stress in breast cancer models. J Nucl Med 58:367–373
6. Ishii T, Sato H, Miura K et al (1992) Induction of cystine transport activity by stress. Ann N Y Acad Sci 663:497–498
7. Hosoya K, Tomi M, Ohtsuki S, Takanaga H, Saeki S, Kanai Y, Endou H, Naito M, Tsuruo T, Terasaki T (2002) Enhancement of the L-cystine transport activity and its relation to xCT gene induction at the blood-brain barrier by diethyl maleate treatment. J Pharmacol Exp Ther 302:225–231
8. Sasaki H, Sato H, Kuriyama-Matsumura K, Sato K, Maebara K, Wang H, Tamba M, Itoh K, Yamamoto M, Bannai S (2002) Electrophile response element – mediated introduction of the cystine/glutamate exchange transporter gene expression. J Biol Chem 277:44765–44771
9. Conrad M, Sato H (2012) The oxidative stress-inducible cystine/glutamate antiporter, system xc-: cystine supplier and beyond. Amino Acids 42:231–246
10. Bridges RJ, Natale NR, Patel SA (2012) System xc- cystine/glutamate antiporter: an update on molecular pharmacology and roles within the CNS. Br J Pharmacol 165:20–34
11. Smolarz K, Krause BJ, Graner FP, Wagner FM, Hultsch C, Bacher-Stier C, Sparks RB, Ramsay S, Fels LM, Dinkelborg LM, Schwaiger M (2013) (S)-4-(3-^{18}F-Fluoropropyl)-L-glutamic acid: an ^{18}F-labeled tumor-specific probe for PET/CT imaging–dosimetry. J Nucl Med 54:861–866
12. Koglin N, Mueller A, Berndt M, Schmitt-Willich H, Toschi L, Stephens AW, Gekeler V, Friebe M, Dinkelborg LM (2011) Specific PET imaging of x_C^- transporter activity using a ^{18}F-labelled glutamate derivative reveals a dominant pathway in tumor metabolism. Clin Cancer Res 17:6000–6011
13. Gout PW, Buckley AR, Simms CR, Bruchovsky N (2001) Sulfasalazine, a potent suppressor of lymphoma growth by inhibition of the xc- cystine transporter: a new action for an old drug. Leukemia 15:1633–1640
14. Müerköster S, Arlt A, Witt M, Gehrz A, Haye S, March C, Grohmann F, Wegehenkel K, Kalthoff H, Fölsch UR, Schäfer H (2003) Usage of the NF-kappa B inhibitor sulfasalazine as sensitizing agent in combined chemotherapy of pancreatic cancer. Int J Cancer 104:469–476
15. Lay JD, Hong CC, Huang JS, Yang YY, Pao CY, Liu CH, Lai YP, Lai GM, Cheng AL, Su IJ, Chuang SE (2007) Sulfasalazine suppresses drug resistance and invasiveness of lung adenocarcinoma cells expressing AXL. Cancer Res 67:3878–3887
16. Narang VS, Pauletti GM, Gout PW, Buckley DJ, Buckley AR (2007) Sulfasalazine induced reduction of glutathione levels in breast cancer cells: enhancement of growth-inhibitory activity of doxorubicin. Chemotherapy 53:210–217
17. Pham AN, Blower PE, Alvarado O, Ravula R, Gout PW, Huang Y (2010) Pharmacogenomic approach reveals a role for the xc- cystine/glutamate antiporter in growth and celastrol resistance of glioma cell lines. J Pharmacol Exp Ther 332:949–958
18. Keam B, Im SA, Kim HJ (2007) Prognostic impact of clinicopathologic parameters in stage II/III breast cancer treated with neoadjuvant docetaxel and doxorubicin chemotherapy: paradoxical features of the triple negative breast cancer. BMC Cancer 7:203
19. Timmerman LA, Holton T, Yuneva M (2013) Glutamine sensitivity analysis indentifies the xCT antiporter as a common triple-negative breast tumour therapeutic target. Cancer Cell 24:450–465
20. Webster JM, Morton CA, Johnson BF, Yang H, Rishel MJ, Lee BD, Miao Q, Pabba C, Yapp DT, Schaffer P (2014) Functional imaging of oxidative stress with a novel PET imaging agent, ^{18}F-5-fluoro-L-aminosuberic acid. J Nucl Med 55:657–664
21. Liefferinge JV, Bentea E, Demuyser T et al (2016) Comparative analysis of antibodies to xCT (SLC7A11): forewarned is forarmed. J Comp Neurol 524:1015–1032
22. Sato H, Tamba M, Ishii T, Bannai S (1999) Cloning and expression of a plasma membrane cystine/glutamate exchange transporter composed of two distinct proteins. J Biol Chem 274:11455–11458
23. Massie A, Schallier A, Mertens B, Vermoesen K, Bannai S, Sato H, Smolders I, Michotte Y (2008) Time-dependent changes in striatal xCT protein expression in hemi-Parkinson rats. Neuroreport 19:1589–1592
24. Burdo J, Dargusch R, Schubert D (2006) Distribution of the cystine/glutamate antiporter system X2c in the brain, kidney, and duodenum. J Histochem Cytochem 54:549–557
25. Shih AY, Erb H, Sun X, Toda S, Kalivas PW, Murphy TH (2006) Cystine/glutamate exchange modulates glutathione supply for neuroprotection from oxidative stress and cell proliferation. J Neurosci 26:10514–10523
26. La Bella V, Valentino F, Piccoli T, Piccoli F (2007) Expression and developmental regulation of the cystine/glutamate exchanger (X2c) in the rat. Neurochem Res 32:1081–1090